Fig.S1

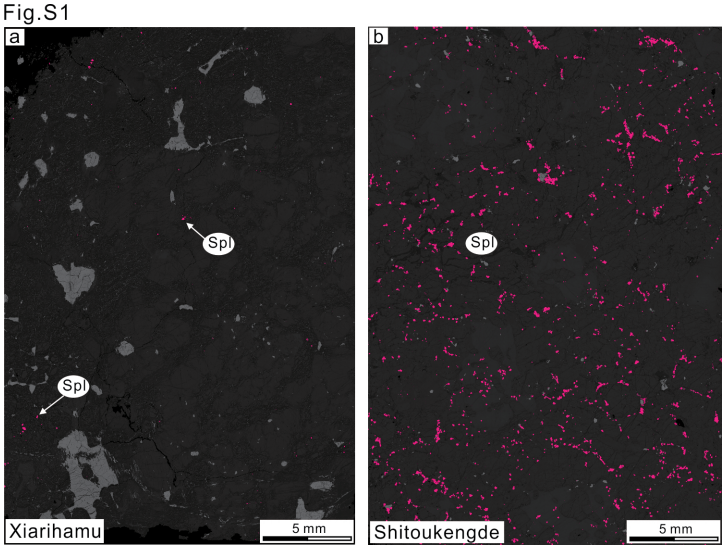

FIGURE S1. The BSE images by TIMA of the Shitoukengde and Xiarihamu intrusions, showing the volume content of the Cr-spinel of the Shitoukengde (~2.32 vol.%) is higher than that of the Cr-spinel in the Xiarihamu lherzolite (~0.05 vol.%).

Fig.S2

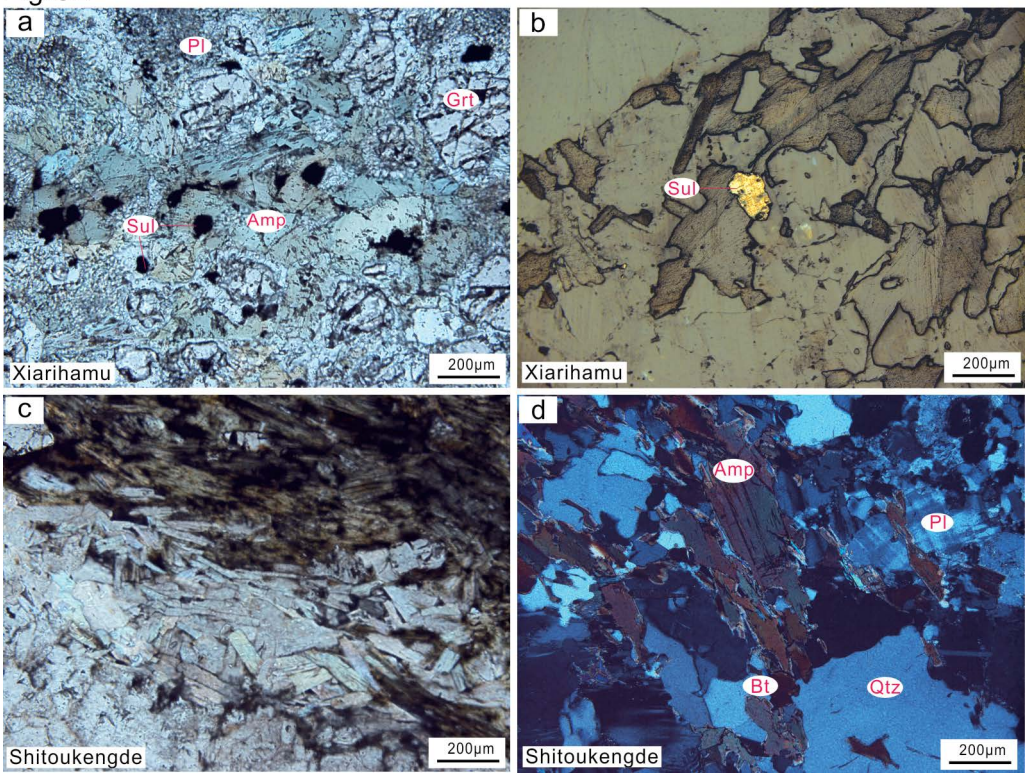

FIGURE S2. Photomicrographs images of country rocks from the Xiarihamu Ni-Cu deposit and Shitoukengde intrusion. Xiarihamu: (a) Amphibole plagiogneiss; (b) Amphibole plagiogneiss contains sulfide grain; Shitoukengde: (c) Amphibole gneiss; (d) Biotite plagiogneiss. Mineral abbreviations: Pl plagioclase, Amp amphibole, Bt biotite, Grt garnet, Qtz quartz, Sul sulfide.

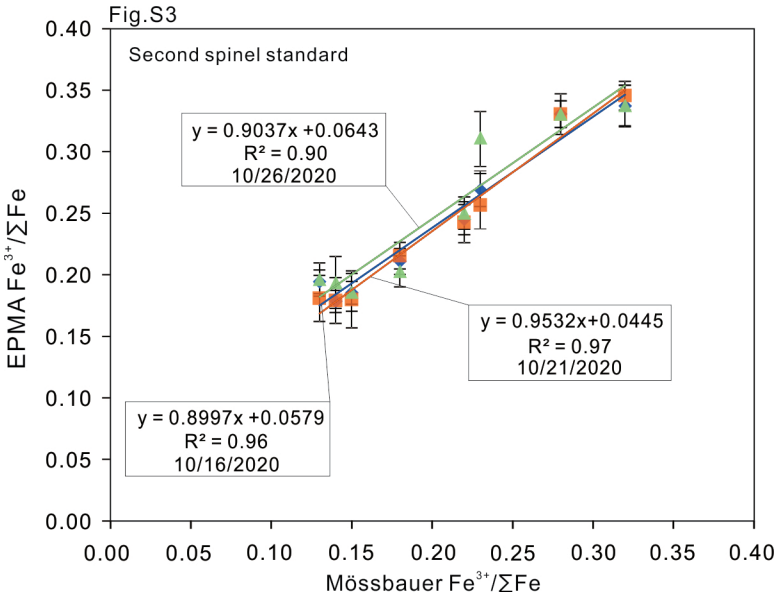

FIGURE S3. Comparison of Cr-spinel $Fe^{3+}/\Sigma Fe$ ratios measured by Mössbauer spectroscopy and EPMA modified by second standard calibration, showing the reproducibility of this method.

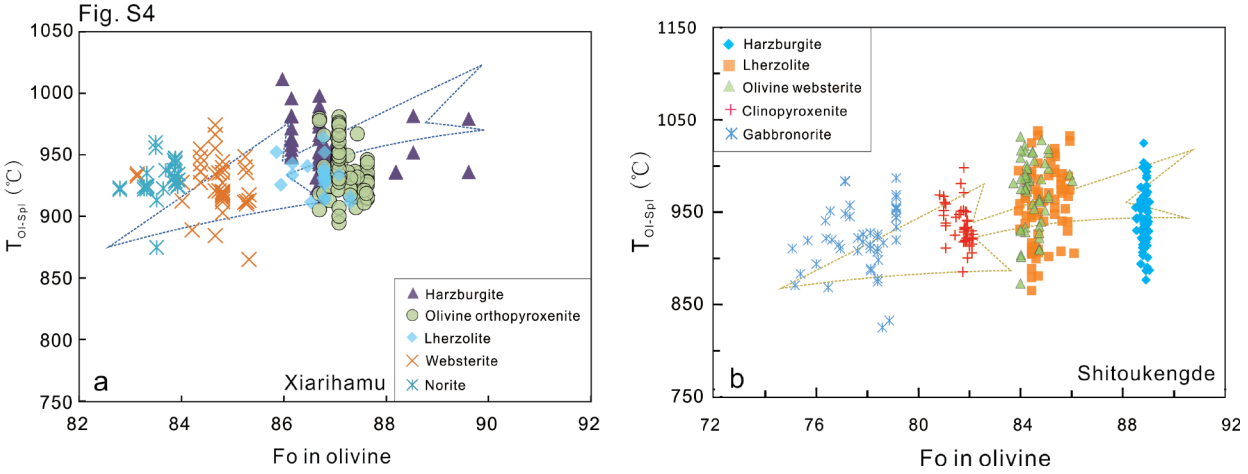

FIGURE S4. Plots of Fo values in olivine versus $T_{Ol\text{-}Spl}$ (°C) for the Xiarihamu Ni-Cu deposit and Shitoukengde intrusion.

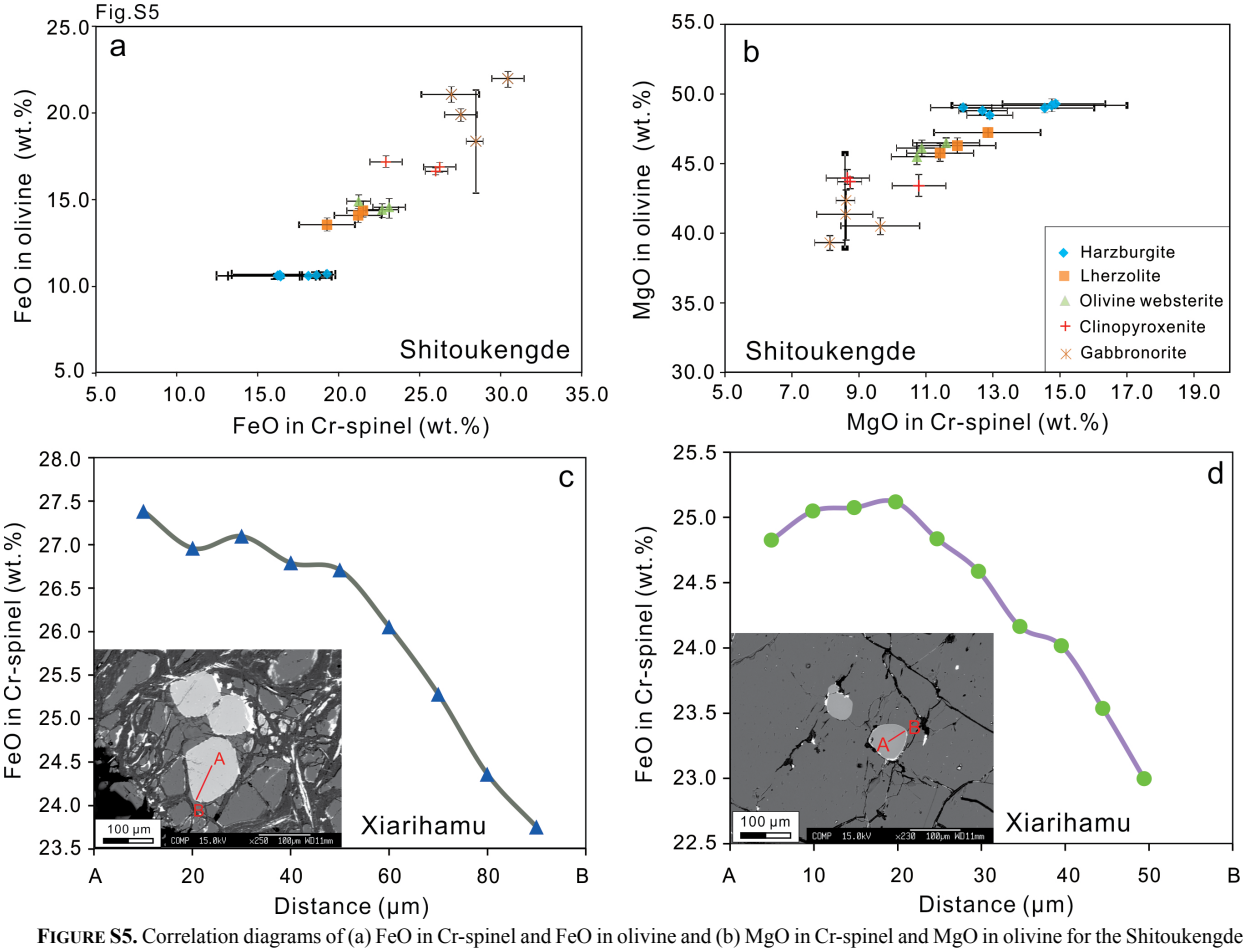

FIGURE S5. Correlation diagrams of (a) FeO in Cr-spinel and FeO in olivine and (b) MgO in Cr-spinel and MgO in olivine for the Shitoukengde intrusion. (c) and (d) show that the FeO contents become lower from core to rim in the individual Cr-spinel grain.

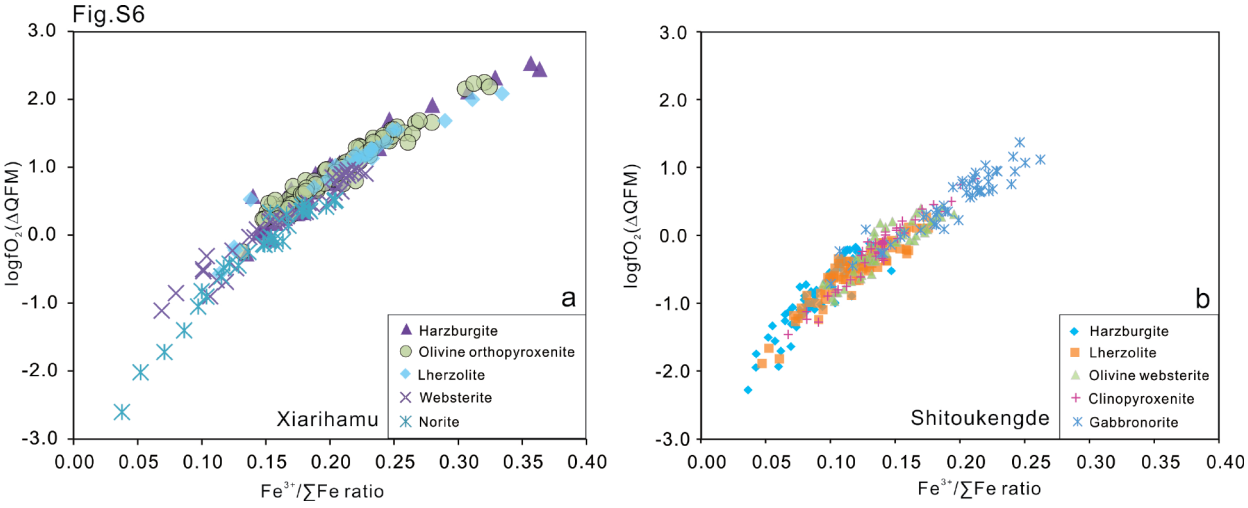

FIGURE S6. Correlation between log fO_2(ΔQFM) and Cr-spinel $Fe^{3+}/\Sigma Fe$ ratio, showing a strong positive correlation between the fO_2 and Cr-spinel $Fe^{3+}/\Sigma Fe$ ratios from the Xiarihamu Ni-Cu deposit and Shitoukengde mafic-ultramafic intrusion.